

Binucleating Aza-Sulfonate and Aza-Sulfinate Macrocycles — Synthesis and Coordination Chemistry

Julia Hausmann,^{[a],[‡]} Steffen Käss,^[a] Sabrina Klod,^[b] Erich Kleinpeter,^[b] and Berthold Kersting*^[a]

Keywords: Cavitands / Macrocyclic ligands / Nickel / S ligands

The preparation and ligating properties of S-oxygenated derivatives of a macrobinucleating hexaazadithiophenolate macrocycle H_2L^1 of the Robson type towards nickel(II) and zinc(II) ions are reported. Nickel complexes of the hexaazadithiophenylsulfonate ligand $(L^2)^{2-}$ [$(L^2)Ni^{II}_2(\mu-L)^+$ ($L = m\text{-Cl-OBz}^-$ (**3**), Cl^- (**4**) and OAc^- (**6**))] are readily obtained in high yields by oxidation of the respective $[(L^1)Ni^{II}_2(\mu-L)]^+$ parent complexes [$L = m\text{-Cl-OBz}^-$ (**2**), Cl^- (**1**), OAc^- (**5**)] with *meta*-chloroperoxybenzoic acid or hydrogen peroxide. Decomposition of the sulfonate complexes gives the free macrocycle H_2L^2 which, upon treatment with $Zn(OAc)_2 \cdot 2H_2O$, produces the diamagnetic zinc complex $[(L^2)Zn^{II}_2(OAc)]^+$ (**8**). A dinuclear Cu^{II} complex of the hexaazadisulfinate derivative $(L^3)^{2-}$,

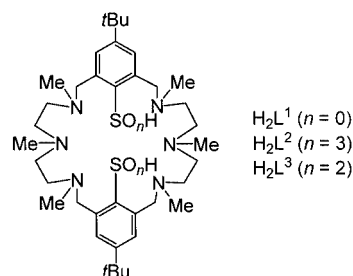
$[(L^3)Cu^{II}_2]^{2+}$ (**9**), is formed rather unexpectedly by air oxidation of $(L^1)^{2-}$ in the presence of Cu^I . The crystal-structure determinations of the perchlorate or tetraphenylborate salts of **2**, **3**, and **4** show that the new ligands support the formation of binuclear complexes with bowl-shaped, calixarene-like binding cavities. NMR spectroscopic studies of **8** show that the complexes retain their solid-state structures in solution. A crystal-structure determination of **9** reveals two five-coordinate Cu^{II} ions bridged by the two sulfinate functions of $(L^3)^{2-}$.

(© Wiley-VCH Verlag GmbH & Co. KGaA, 69451 Weinheim, Germany, 2004)

Introduction

The development of ligand systems that support the formation of metal complexes with confined environments about active coordination sites is currently attracting much interest.^[1–3] This is mainly due to the fact that such assemblies improve the ability to control the rate and selectivity of substrate transformations.^[4–8] Such aggregates also allow for the construction of more-effective enzyme mimics.^[9] Consequently, a large number of bowl-shaped supporting ligands have been reported and their ligating properties towards the 3d elements have been investigated. While most of these ligands form mononuclear complexes, as, for instance, the calixarenes,^[10] the cyclodextrins,^[11] and some tripod ligands,^[12–14] there are only a few reports of ligand systems that impose calixarene-like structures about dinuclear cores.^[15–17] We have recently shown that N-functionalized hexaazadithiophenolate macrocycles^[18,19] of the Robson type^[20–23] are suitable for the construction of such

species.^[24] The unique features of the corresponding complexes^[25] led us to investigate potential routes to S-oxygenated derivatives of H_2L^1 and to examine the ligating properties of these hitherto unknown ligand systems (Scheme 1). Herein we report the synthesis of the binucleating hexaazasulfonate ligand $(L^2)^{2-}$ and demonstrate its ability to form dinuclear transition-metal complexes with bowl-shaped binding cavities. The synthesis and crystal structure of a dinuclear copper(II) complex of the related hexaazasulfinate ligand $(L^3)^{2-}$ are also reported.



Scheme 1. Structures of the ligands H_2L^1 , H_2L^2 and H_2L^3 (see Scheme 2 for numbering of complexes)

Results and Discussion

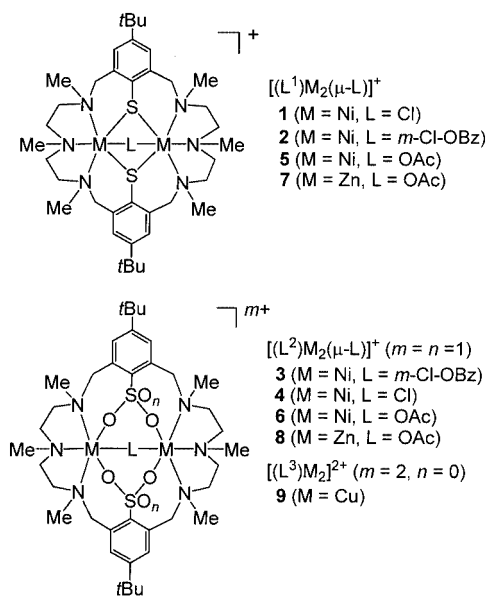
The compounds synthesized in this paper are collected in Scheme 2. Of these, the nickel and zinc complexes **1**, **5**, and **7** have been reported previously.

^[a] Institut für Anorganische und Analytische Chemie, Universität Freiburg
Albertstr. 21, 79104 Freiburg, Germany
Fax: (internat.) + 49-761-203-5987
E-mail: berthold.kersting@ac.uni-freiburg.de

^[b] Institut für Chemie, Universität Potsdam
P. O. Box 601553, 14415 Potsdam, Germany

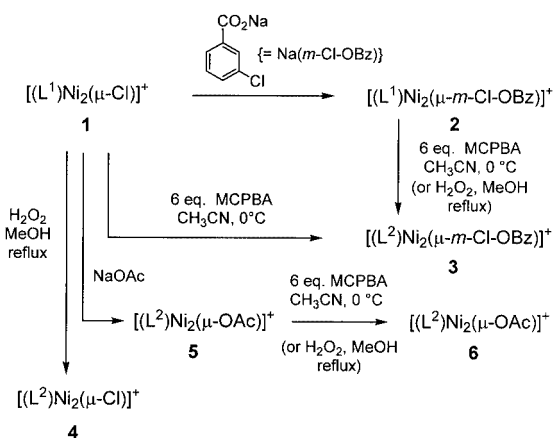
^[‡] Present address: Department of Chemistry, University of Otago
P. O. Box 56, Dunedin, New Zealand

Supporting information for this article is available on the WWW under <http://www.eurjic.org> or from the author.



Scheme 2. Synthesized complexes and their labels (see Scheme 1 and ref. 31 for ligand abbreviations)

Attempts to *S*-oxygenate the free hexaazadithiophenol H_2L^1 invariably proved unsuccessful, presumably due to the formation of amine *N*-oxides. The oxidation of dinickel complexes of $(L^1)^{2-}$ was attempted next, since this has recently been demonstrated to be a versatile method for the preparation of sulfonate complexes,^[26] even for complexes of labile transition-metal ions such as nickel(II).^[27–29] In a preliminary experiment the *meta*-chlorobenzoato-bridged species **2**^[30] was treated with six equivalents of *meta*-chloroperoxybenzoic acid (MCPBA) at 0 °C (Scheme 3).^[31] This resulted in the rapid and almost quantitative formation of the desired aminosulfonate complex **3**. The facile formation of **3** is somewhat remarkable given that *S*-oxygenation of bridging thiolate functions has not been observed previously in nickel thiolate chemistry.^[32,33]



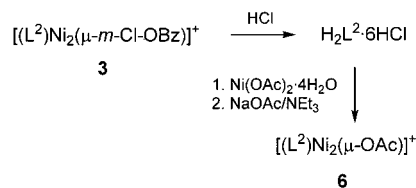
Scheme 3. Synthesis of compounds 2–6

In light of these results the oxidation of the chloro- and acetato-bridged species **1** and **5**, respectively, was examined next (Scheme 3). The oxidation of the chloro complex **1** by

MCPBA was expected to give the μ -Cl compound **4**, but the infrared spectrum (vide infra) revealed the presence of the μ -*meta*-chlorobenzoate-containing complex **3**, showing that this transformation is accompanied by a substitution of the bridging chloride ion by the *meta*-chlorobenzoate group (which is produced upon reduction of MCPBA). In contrast, the oxidation of **5** yields the acetato-bridged complex **6** as the sole product. Thus, in this case an exchange of the encapsulated acetate moiety by the external *meta*-chlorobenzoate does not occur, despite it being present in a sixfold molar excess.

In the course of our work it was found that the aminosulfonate complexes **3** and **6** can also be prepared by oxidation of their respective parent complexes with hydrogen peroxide (Scheme 3). This prompted us to test whether complex **4** would be similarly accessible by H_2O_2 oxidation of **1**. Indeed, treatment of **1** with a large excess of H_2O_2 resulted in the formation of a pale-green solution, from which the desired μ -chloro complex **4**·ClO₄ could be obtained upon addition of an excess of LiClO₄. Nevertheless, the thiolate complexes are very resistant towards oxidation by H_2O_2 . In the case of **2** and **5**, for example, a large excess and prolonged heating was required to obtain the respective oxidation products **3** and **6** in good yields.

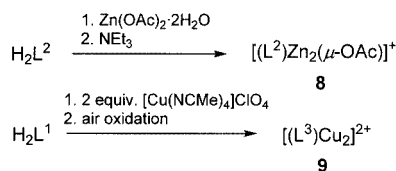
As noted above, the direct oxidation of H_2L^1 failed to provide the macrocyclic hexaazadisulfonic acid H_2L^2 , and so another route had to be developed. We have previously observed that binuclear complexes of the aminothiolate ligand $(L^1)^{2-}$ decompose under acidic conditions to give the free aminothiol H_2L^1 as its hexahydrochloride salt.^[34] Accordingly, the decomposition of the perchlorate salt **3**·ClO₄ with hydrochloric acid was attempted (Scheme 4). The aminosulfonate complex was found to be very stable under acidic conditions, but with concentrated hydrochloric acid complete hydrolysis occurred, such that the desired ligand H_2L^2 ·6HCl could be isolated in good yields. The identity of H_2L^2 ·6HCl was confirmed by IR, ¹H and ¹³C NMR spectroscopy (see below), and by the successful regeneration of complex **6**. Thus, treatment of H_2L^2 ·6HCl with two equivalents of Ni(OAc)₂·4H₂O resulted in a pale-green solution, from which the known complex **6**·ClO₄ could be isolated in excellent yields upon addition of LiClO₄.



Scheme 4. Synthesis of compounds H_2L^2 ·6HCl and **6**

In order to get some preliminary information on the solution structures of the new complexes, the synthesis of diamagnetic zinc complexes was devised. The acetato-bridged dizinc complex **8** was selected as the target compound. All attempts to access **8** by oxidation of its parent complex **7** were unsuccessful, but, similar to **6**·ClO₄, this complex

could be readily prepared by the complexation of the free macrocycle with $\text{Zn}(\text{OAc})_2 \cdot 2\text{H}_2\text{O}$ (Scheme 5). Thus, the reaction of $\text{H}_2\text{L}^2 \cdot 6\text{HCl}$ with two equivalents of $\text{Zn}(\text{OAc})_2 \cdot 2\text{H}_2\text{O}$ resulted in a colourless solution, from which the colourless perchlorate salt $[(\text{L}^2)\text{Zn}_2(\mu\text{-OAc})]\text{ClO}_4$ ($8 \cdot \text{ClO}_4$) was obtained in the form of large crystals in nearly quantitative yield upon addition of LiClO_4 .



Scheme 5. Synthesis of compounds **8** and **9**

Finally, we were also able to prepare a dinuclear complex of the aminosulfonate ligand $(\text{L}^3)^{2-}$, the dicopper(II) complex **9**. This complex was obtained rather unexpectedly from attempts to prepare mixed-valent $\text{Cu}^{\text{I}}\text{Cu}^{\text{II}}$ complexes of $(\text{L}^1)^{2-}$. Attempts to access this compound by air oxidation of a methanolic solution of the dicopper(I) complex $[(\text{L}^1)\text{Cu}^{\text{I}}_2]^{2-}$ (prepared in situ from H_2L^1 , $[\text{Cu}^{\text{I}}(\text{CH}_3\text{CN})_4](\text{ClO}_4)$ and NEt_3), however, resulted in the formation of the sulfinate complex **9** instead. The dark-green perchlorate salt $[(\text{L}^3)\text{Cu}^{\text{II}}_2](\text{ClO}_4)_2$ [**9**·(ClO_4)₂] was reproducibly obtained as a dark-green microcrystalline solid in about 45% yield.

All new complexes are stable in air, both in solution and in the solid state. The perchlorate salts are very soluble in a range of common organic solvents. The solubility of the complexes of the hexaazadisulfonate macrocycle is particularly good in polar protic solvents such as ethanol, methanol, and even 25% aqueous methanol. In contrast to the aminothiolate complexes, the sulfonate complexes are stable over a wide pH range. They can be isolated from acidic or basic methanolic solution (pH 1 to 10) without any noticeable decomposition or exchange of the bridging coligands L. The new compounds gave satisfactory elemental analyses and were characterized by spectroscopic methods (IR, UV/Vis, ^1H and ^{13}C NMR spectroscopy) and compounds

2· $\text{BPh}_4 \cdot 1.25\text{MeCN}$, **3**· $\text{BPh}_4 \cdot 4\text{EtOH} \cdot 2\text{H}_2\text{O}$, **4**· $\text{BPh}_4 \cdot \text{EtOH} \cdot 0.5\text{CH}_3\text{CN}$, and **9**·(ClO_4)₂· H_2O also by X-ray structure analysis.

Infrared and UV/Vis Spectroscopy

Table 1 summarizes selected analytical data for compounds **1–9**. In agreement with the formulation of **3** the IR spectrum displays a strong band at 1220 cm^{-1} for the sulfonate group $\nu(\text{RSO}_3^-)$ ^[35] and two absorptions at 1563 cm^{-1} [$\nu_{\text{as}}(\text{RCO}_2^-)$] and 1410 cm^{-1} [$\nu_{\text{s}}(\text{RCO}_2^-)$] for the *meta*-chlorobenzoate coligand.^[36] The latter two values are very similar to those of the parent complex **2**, suggesting that the *meta*-chlorobenzoate moiety in **3** is also in the $\mu_{1,3}$ -bridging mode. Similarly, the IR spectrum of the acetato-bridged complex **6** shows distinct IR bands for bridging acetate (1597 and 1411 cm^{-1}) and sulfonate groups (1202 cm^{-1}). Unfortunately, the sulfonate stretching frequencies overlap with the bands of the $[(\text{L}^2)\text{Ni}^{\text{II}}_2]^{2+}$ fragment^[37] and the counterions (ClO_4^- or BPh_4^-), such that the coordination mode of the RSO_3^- functions could not be deduced from the IR data. The IR spectra of the homologous nickel and zinc complexes **5** and **7** (and **6** and **8**) are identical. Finally, the IR spectrum of the copper complex **9** shows two absorptions at 1052 and 950 cm^{-1} , which can be attributed to the stretching frequencies of the sulfinate functions.^[38] Again, the coordination mode of the sulfinate groups could not be inferred from the IR data.

All new complexes were further characterized by UV/Vis spectroscopy. The UV/Vis data of **1**, **2** and **5** have been reported previously.^[24,25] The electronic absorption spectra of the new complexes were recorded in the range $300\text{--}1600\text{ nm}$ in acetonitrile solution at ambient temperature (Table 1). The spectra of the pale-green nickel complexes **3**, **4**, and **6** are similar but not identical. In agreement with the oxidation of the thiophenolate sulfur atoms, there are no intense $\text{RS}^- \rightarrow \text{Ni}^{\text{II}}$ charge-transfer transitions in the 300 to 400 nm region.^[39] Each compound displays three weak absorption bands. The first band is seen around 400 nm , the second one appears in the 670 to 690 nm range, and the third one is observed between 1120 and 1130 nm . These absorptions can be attributed to the three spin-allowed d-d-transitions $\nu_3\text{ }[{}^3A_{2g}(F) \rightarrow {}^3T_{1g}(P)]$, $\nu_2\text{ }[{}^3A_{2g}(F) \rightarrow$

Table 1. Selected analytical data of compounds **2–9**^[a]

Compound	IR bands (cm^{-1}) and assignments	UV/Vis λ_{max} [nm] ($\epsilon\text{ [M}^{-1}\text{cm}^{-1}]$)
1		390 (2830), 625 (58), 941 (56) ^[b]
2	1566, 1423; $\nu_{\text{as}}, \nu_{\text{s}}(\text{RCO}_2^-)$	385 (2400), 651 (26), 1116 (65)
3	1563, 1410; $\nu_{\text{as}}, \nu_{\text{s}}(\text{RCO}_2^-)$; 1220 cm^{-1} $\nu_{\text{s}}(\text{RSO}_3^-)$	400 (47), 674 (14), 1126 (15)
4	1202 cm^{-1} $\nu_{\text{s}}(\text{RSO}_3^-)$	396 (33), 686 (15), 1124 (17)
5	1588, 1426; $\nu_{\text{as}}, \nu_{\text{s}}(\text{RCO}_2^-)$ ^[c]	395 (2640), 649 (28), 1134 (55) ^[c]
6	1597, 1411; $\nu_{\text{as}}, \nu_{\text{s}}(\text{RCO}_2^-)$; 1202 cm^{-1} $\nu_{\text{s}}(\text{RSO}_3^-)$	398 (55), 670 (25), 1122 (47)
$\text{H}_2\text{L}^{\text{Me}^+} \cdot 6\text{HCl}$	1228 cm^{-1} $\nu(\text{RSO}_3\text{H})$	
7	1585, 1428; $\nu_{\text{as}}, \nu_{\text{s}}(\text{RCO}_2^-)$ ^[c]	
8	1595, 1411; $\nu_{\text{as}}, \nu_{\text{s}}(\text{RCO}_2^-)$; 1202 cm^{-1} $\nu_{\text{s}}(\text{RSO}_3^-)$	
9	$1052, 950\text{ cm}^{-1}$ $\nu_{\text{s}}(\text{RSO}_2^-)$	668 (430), 947 (153)

^[a] The complexes were isolated as their ClO_4^- or BPh_4^- salts. ^[b] Ref.^[24a] ^[c] Ref.^[25]

$^3T_{1g}(F)$], and ν_1 [$^3A_{2g}(F) \rightarrow ^3T_{2g}(F)$], respectively, of an octahedral d^8 nickel(II) ion. The higher energy features below 300 nm result from $\pi-\pi^*$ transitions within the $(L^2)^{2-}$ ligand. The slight differences in the position of the d-d transitions indicate that each complex retains its coligand in the solution state. Finally, the dark-green dicopper(II) complex displays a single absorption band at 668 nm. This is a typical value for square-pyramidal $Cu^{II}N_3O_2$ complexes.^[40]

NMR Spectroscopy

To investigate the solution structures, the zinc complex **8** was characterized by 1H and ^{13}C NMR spectroscopy. The NMR spectroscopic properties of the zinc complex **7** have been reported previously.^[25] The 1H NMR spectrum of **8** in CD_3CN solution displays only one set of signals, indicating that **8** exists as a single isomer in solution. The four aromatic protons, the methyl protons on the benzylic nitrogens, the methyl protons on the central amine nitrogen of the linking diethylene triamine units, and the *tert*-butyl protons all appear as singlets. This is indicative of a C_{2v} symmetric solution structure for the $[(L^2)Zn_2(\mu-OAc)]^+$ cation. In agreement with this assumption the $[(L^2)Zn_2]^{2+}$ fragment gives rise to only eleven ^{13}C NMR signals (seven for the aliphatic and four for the aromatic carbon atoms). The appearance of a 1H NMR signal at $\delta = 0.59$ ppm, which can be assigned to the methyl protons of the bridging acetate ion, is worthy of note. The observed high-field shift [**8**: $\Delta\delta = -1.24$ ppm, relative to NaOAc ($\delta = 1.83$ ppm)] can be explained by the ring current. As can be seen from Figure S1,^[41] the methyl protons of the coordinated acetate group are positioned above the center of the two phenyl rings in the shielding region. The angle between the phenyl rings in **8** (41.6°)^[42] is more acute than in **7** (80.0°) and hence the shielding effect is less pronounced in the latter (**7**: $\Delta\delta = -0.92$ ppm, relative to NaOAc). This is also supported by

preliminary chemical shielding calculations using Gaussian 98 ($\Delta\delta_{calc} = -1.92$ ppm for **8** vs. -1.25 ppm for **7**; see Exp. Sect. for details).

X-ray Crystallography

Although the formulations of the new compounds were reasonably substantiated by the above spectroscopic data, further confirmation was provided by X-ray diffraction studies. Single crystals of X-ray quality were obtained for the perchlorate or tetraphenylborate salts of complexes **2**, **3**, **4**, and **9**. The crystal structures of complexes **1**, **5**, and **7** have been reported previously.^[24,25] All data collections were performed at 210 K. A common labeling scheme for the $[(L^1)Ni_2]^{2+}$ and $[(L^2)Ni_2]^{2+}$ units has been used to facilitate structural comparisons. Selected bond lengths and angles are given in Table 2 and 3.

Table 3. Selected bond lengths (Å) and angles ($^\circ$) in complex **9**; symmetry code used to generate equivalent atoms ($'$): $-x, -y, -z$

Cu(1)–O(1)	2.002(2)	Cu(1)–O(2')	1.968(2)
Cu(1)–N(1)	2.258(3)	Cu(1)–N(2)	2.056(3)
Cu(1)–N(3)	2.041(3)	S(1)–O(1)	1.504(2)
S(1)–O(2)	1.510(3)	Cu(1)···Cu(1')	4.993(1)
O(2')–Cu(1)–O(1)	95.91(10)	O(2')–Cu(1)–N(1)	96.36(11)
O(2')–Cu(1)–N(3)	89.81(12)	O(1)–Cu(1)–N(1)	88.38(11)
O(1)–Cu(1)–N(3)	154.03(11)	N(3)–Cu(1)–N(1)	116.20(12)
O(2')–Cu(1)–N(2)	175.42(12)	N(2)–Cu(1)–N(1)	85.12(13)
O(1)–Cu(1)–N(2)	88.45(12)	O(1)–S(1)–O(2)	109.46(14)
N(3)–Cu(1)–N(2)	85.65(12)		

The structure of **2** (Figure 1) reveals the presence of discrete dinuclear $[(L^1)Ni_2(m-Cl-OBz)]^+$ cations, tetraphenylborate anions and acetonitrile molecules of solvent of crystallization. The macrocycle $(L^1)^{2-}$ adopts a conical calixarene-like conformation, which is typical for carboxylato-

Table 2. Selected bond lengths (Å) and angles ($^\circ$) in complexes **2**, **3**, and **4**

2 ^[a]		3		4 ^[a]	
Ni(1A)–O(1A)	2.010(3) [2.028(3)]	Ni(1)–O(1)	2.111(5)	Ni(1A)–Cl(1A)	2.439(1) [2.482(2)]
Ni(1A)–N(1A)	2.282(3) [2.281(3)]	Ni(1)–N(1)	2.230(7)	Ni(1A)–N(1A)	2.160(4) [2.183(4)]
Ni(1A)–N(2A)	2.176(4) [2.158(3)]	Ni(1)–N(2)	2.136(6)	Ni(1A)–N(2A)	2.146(4) [2.132(4)]
Ni(1A)–N(3A)	2.222(4) [2.239(3)]	Ni(1)–N(3)	2.265(6)	Ni(1A)–N(3A)	2.320(4) [2.264(4)]
Ni(1A)–S(1A)	2.504(2) [2.512(1)]	Ni(1)–O(5)	2.073(5)	Ni(1A)–O(1A)	2.064(3) [2.048(3)]
Ni(1A)–S(2A)	2.406(2) [2.396(1)]	Ni(1)–O(7)	2.040(5)	Ni(1A)–O(4A)	2.051(3) [2.095(3)]
Ni(2A)–O(2A)	2.020(3) [2.016(3)]	Ni(2)–O(2)	2.102(5)	Ni(2A)–Cl(1A)	2.453(1) [2.449(1)]
Ni(2A)–N(4A)	2.207(4) [2.216(3)]	Ni(2)–N(4)	2.266(6)	Ni(2A)–N(4A)	2.180(4) [2.254(4)]
Ni(2A)–N(5A)	2.170(4) [2.172(3)]	Ni(2)–N(5)	2.131(7)	Ni(2A)–N(5A)	2.120(4) [2.132(4)]
Ni(2A)–N(6A)	2.307(4) [2.311(3)]	Ni(2)–N(6)	2.254(7)	Ni(2A)–N(6A)	2.286(4) [2.195(4)]
Ni(2A)–S(1A)	2.484(2) [2.501(2)]	Ni(2)–O(4)	2.109(5)	Ni(2A)–O(2A)	2.057(3) [2.043(4)]
Ni(2A)–S(2A)	2.401(2) [2.398(1)]	Ni(2)–O(8)	2.009(5)	Ni(2A)–O(5A)	2.098(3) [2.084(3)]
Ni–N ^[b]	2.227(3) [2.230(3)]		2.214(7)		2.202(4) [2.193(4)]
Ni–O ^[b]	2.015(3) [2.022(3)]		2.074(5)		2.068(3) [2.068(3)]
Ni–S ^[b]	2.449(2) [2.451(1)]				
C(4)···C(20)	9.489 [9.563]		7.958		9.471 [9.370]
Ph/Ph ^[c]	93.6 [92.2]		44.5		72.2 [69.8]
Ni···Ni	3.460(1) [3.457(1)]		4.584(2)		4.063(2) [4.086(2)]

^[a] There are two crystallographically independent molecules A and B in the unit cell. Values in square brackets refer to the corresponding bond lengths of the second molecule. ^[b] Average values. ^[c] Angle between the normals of the planes of the two aryl rings.

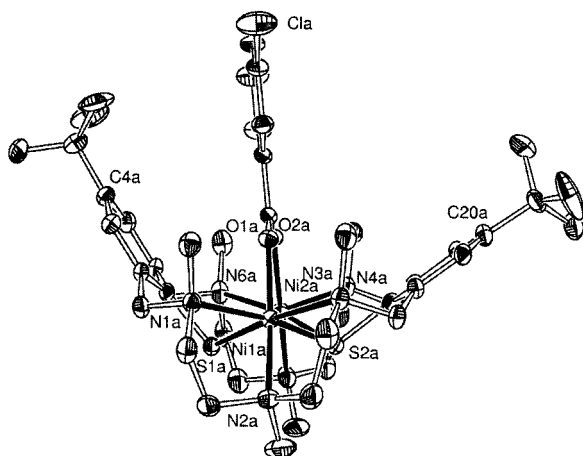


Figure 1. Molecular structure of the cation **2**; thermal ellipsoids are drawn at the 30% probability level; hydrogen atoms are omitted for clarity.

bridged complexes of this ligand.^[43] In this approximately C_{2v} -symmetric structure, the two nickel(II) ions are coordinated in a square-pyramidal fashion by the two *fac*- $N_3(\mu-S)_2$ donor sets of the macrocycle. Upon coordination of the *meta*-chlorobenzoate group, both nickel atoms reach distorted octahedral coordination environments at a metal–metal distance of 3.460(1) Å. As in previously reported carboxylato-bridged nickel complexes of $(L^1)^{2-}$, the Ni–N bond lengths involving the four benzylic nitrogen donors are invariably longer (by ca. 0.10–0.12 Å) than the ones comprising the central nitrogen atoms of the linking diethylenetriamine units. The individual Ni–S distances also vary considerably. These distortions are almost certainly a consequence of the steric constraints of the macrocycle.

The dimensions of the bowl-shaped binding cavity of the $[(L^1)Ni_2]^{2+}$ fragment can be described by the intramolecular distance between the two opposing aryl ring carbon atoms C(4) and C(20) and by the angle between the planes through the phenyl rings. For the present structure, the corresponding values are 9.489(1) Å and 93.6°, respectively. As we will show below, these values decrease considerably upon oxygenation of the thiophenolate sulfur atoms.

The crystal-structure determination of **3**·BPh₄ unambiguously confirmed **3** to be a bioctahedral dinickel complex of the new hexaazadiphenylsulfonate ligand $(L^2)^{2-}$ (see Figure 2). The two sulfonate groups and the *meta*-chlorobenzoate ion bridge the two Ni^{II} ions in symmetrical $\mu_{1,3}$ -modes, at a distance of 4.584(1) Å. The amine nitrogens of $(L^2)^{2-}$ occupy the remaining positions and complete the pseudo-octahedral N_3O_3 coordination spheres of the metal ions. Precedents for this type of $\mu_{1,3}$ -bridging RSO_3^- functions exist in the literature,^[44] albeit not incorporated into a macrobinucleating ligand. A comparison with the structure of the parent complex **2** reveals a significant compression of the binding pocket. Thus, in **3** the best planes through the phenyl rings intersect at an angle of 44.6°. This value is much more acute than in **2** (93.6°). As a consequence the *meta*-chlorobenzoate ion becomes tightly embraced by the

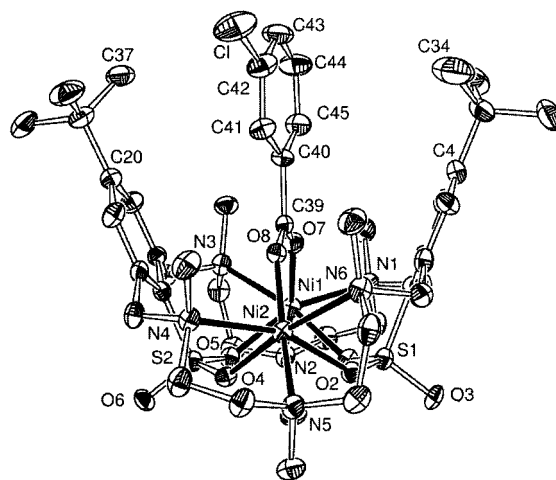


Figure 2. Molecular structure of the cation **3**; thermal ellipsoids are drawn at the 30% probability level; hydrogen atoms are omitted for clarity.

tertiary butyl groups of $(L^2)^{2-}$, as evidenced by a very short C(4)···C(20) distance of 7.958 Å. The short distances between the coligand and the *t*Bu protons [H(37a)···C(43) 3.230 Å; H(34c)···C(43) 3.311 Å] are indicative of intramolecular van der Waals interactions between the host and its guest. This is also supported by the wider binding pocket in the μ -Cl species **4** (see below).

Crystals of **4**·BPh₄·EtOH·0.5CH₃CN are composed of discrete, dinuclear $[(L^2)Ni_2(\mu-Cl)]^+$ cations, tetraphenylborate anions and ethanol and acetonitrile molecules of solvent of crystallization (see Figure 3). Similar to **3**, the aminosulfonate ligand in **4** assumes a calixarene-like conformation such that the bridging halide ion is deeply buried in the binding cavity of the $[(L^2)Ni_2]^{2+}$ fragment. This ligand conformation is different from the “partial cone”-like conformation seen in its parent **1**.^[24] The corresponding Ni–O and Ni–N bond lengths in **3** and **4**, respectively, are very similar. In both structures the Ni–N bond lengths involving the four benzylic nitrogen donors are invariably longer (by ca. 0.1 Å) than the ones comprising the central nitrogen atoms of the linking diethylenetriamine units; the Ni–O distances also vary considerably. These distortions can be traced back to the steric constraints of the macrocycle. The main differences between the structures of **3** and **4** concern the Ni···Ni distances (4.063 Å in **4**, 4.584 Å in **3**) and the angle between the phenyl rings (72.2° in **4**, 44.5° in **3**). While the differences in the Ni···Ni distances can be traced back to the different ligating properties of the coligands, the more pronounced clipping of the phenyl rings in **3** is presumably due to attractive van der Waals interactions between the apolar CH function of the bowl-shaped host and its guest. Such secondary interactions are of importance as they can confer unusual binding modes on the coligands.^[45]

Finally, the crystal structure determination of **9**·(ClO₄)₂·H₂O reveals the dication **9** to be a dicopper(II) complex of the new hexaazadiphenylsulfonate ligand $(L^3)^{2-}$. The complex dication exhibits a center of inversion such that the asymmetric unit consists of only one half of the

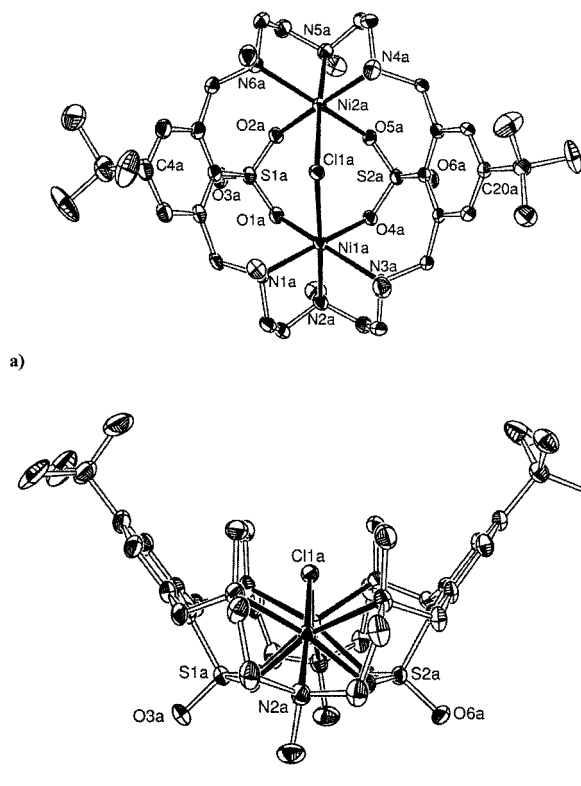


Figure 3. Two views of the molecular structure of the cation **4**; thermal ellipsoids are drawn at the 30% probability level; hydrogen atoms are omitted for clarity

formula unit. As can be seen from Figure 4 the two sulfinate functions bridge the two Cu^{II} ions in symmetrical $\mu_{1,3}$ -modes, at a $\text{Cu}\cdots\text{Cu}$ distance of 4.993(1) Å. The amine nitrogens of $(\text{L}^3)^{2-}$ occupy the remaining positions and complete the pseudo-square-pyramidal N_3O_2 coordination spheres of the metal ions. The mean $\text{Cu}-\text{N}$ and $\text{Cu}-\text{O}$ distances of 2.118 and 1.985 Å show no unusual features and compare well with those in related $\text{Cu}^{\text{II}}\text{N}_3\text{O}_2$ complexes.^[46]

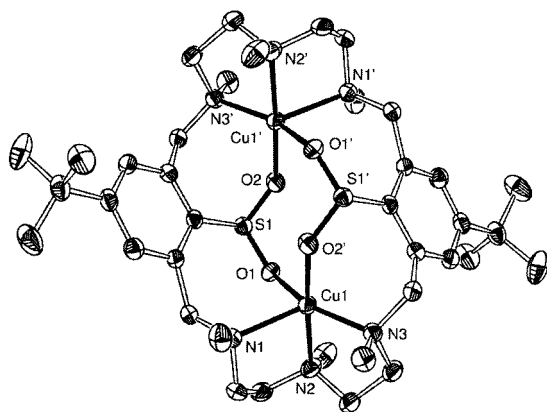


Figure 4. Molecular structure of the dication **9**; thermal ellipsoids are drawn at the 50% probability level; hydrogen atoms are omitted for clarity

Conclusion

The main findings of the present work can be summarized as follows: a) S-oxygenated derivatives of binucleating hexaazadithiophenolate macrocycles of the Robson type can be readily prepared by oxidation of dinuclear nickel complexes of the parent hexaazadithiophenolate macrocycles followed by decomposition of the oxidation products in acidic solution. b) The new hexaazadisulfonate macrocycle $(\text{L}^2)^{2-}$ is an effective dinucleating ligand that supports the formation of dinuclear complexes of the type $[(\text{L}^2)\text{M}_2(\mu\text{-L})]^+$ with a bowl-shaped, calixarene-like structure. c) The $[(\text{L}^2)\text{M}_2]^{2+}$ fragment is capable of binding different coligands. d) The $[(\text{L}^2)\text{M}_2(\mu\text{-L})]^+$ complexes retain their solid-state structures in the solution state. e) The more pronounced clipping of the phenyl rings in the $[(\text{L}^2)\text{M}_2(\mu\text{-L})]^+$ complexes is presumably due to attractive van der Waals interactions between the ligand matrix of the complex and the encapsulated coligand. f) The sulfonate complexes are stable over a wider pH range and oxidizing conditions. Thus, the reactivity of the encapsulated coligands can now also be examined under these more forcing conditions.

Experimental Section

General: Unless otherwise noted the preparations of the metal complexes were carried out under an argon atmosphere by using standard Schlenk techniques. The compounds $\text{H}_2\text{L}^1\cdot 6\text{HCl}$, $[(\text{L}^1)\text{Ni}_2(\text{Cl})]\text{ClO}_4$ (**1**· ClO_4), $[(\text{L}^1)\text{Ni}_2(\text{OAc})]\text{ClO}_4$ (**5**· ClO_4), and $[(\text{L}^1)\text{Zn}_2(\text{OAc})]\text{ClO}_4$ (**7**· ClO_4) were prepared as described in the literature.^[25] All other compounds and reagents were purchased from Aldrich. Melting points were determined in capillaries and are uncorrected. ^1H and ^{13}C NMR spectra were recorded on a Bruker AVANCE DPX-200 or a Varian 300 unity spectrometer. Elemental analyses were performed on a Vario EL analyzer (Elementaranalysesysteme GmbH). All compounds crystallize with solvent molecules (see crystal structures of **3**· $\text{BPh}_4\cdot 2\text{EtOH}\cdot 0.5\text{CH}_3\text{CN}$ and **4**· $\text{BPh}_4\cdot 2\text{EtOH}\cdot 0.5\text{CH}_3\text{CN}$), but the compounds slowly lose their solvent molecules of crystallization upon standing in air. This is why the observed microanalytical data do not fit exactly with the calculated values (for the solvent-free compounds). IR spectra were recorded on a Bruker VECTOR 22 FT-IR spectrophotometer as KBr pellets. Electronic absorption spectra were recorded on a Jasco V-570 UV/Vis/near IR spectrophotometer.

Safety note! Perchlorate salts of transition-metal complexes are hazardous and may explode. Only small quantities should be prepared and great care taken. We have not encountered any problems with the ClO_4 salts of the present complexes (hammer test), and have for this reason not prepared the BF_4 complexes.

$[(\text{L}^1)\text{Ni}^{\text{II}}_2(m\text{-Cl-OBz})]\text{ClO}_4$ (2**· ClO_4):** A solution of sodium *meta*-chlorobenzoate (26.8 mg, 0.150 mmol) in methanol (5 mL) was added to a solution of $[(\text{L}^1)\text{Ni}_2(\text{Cl})]\text{ClO}_4$ (92 mg, 0.10 mmol) in methanol (30 mL). The mixture was stirred for 2 h, during which time the color of the solution turned from yellow to pale green. A solution of $\text{LiClO}_4\cdot 3\text{H}_2\text{O}$ (400 mg, 2.50 mmol) in methanol (2 mL) was then added. The resulting pale-green microcrystalline solid was isolated by filtration, washed with methanol, and dried in air. This material was recrystallized once from a mixed ethanol/acetonitrile (1:1) solvent system. Yield: 78 mg (75%). M.p. 348–350 °C (de-

comp.). UV/Vis (CH_3CN): λ_{max} (ϵ) = 385 (2400), 651 (26), 1116 nm ($65 \text{ M}^{-1}\text{cm}^{-1}$). IR (KBr): $\tilde{\nu}$ = 1598 cm^{-1} , 1566 s [$\nu_{\text{as}}(\text{RCO}_2^-)$], 1423 s [$\nu_{\text{s}}(\text{RCO}_2^-)$], 1098 vs [$\nu(\text{ClO}_4^-)$]. The tetraphenylborate salt $[(\text{L}^1)\text{Ni}^{II}_2(m\text{-Cl-OBz})]\text{BPh}_4$ (**2-BPh₄**) was prepared by adding NaBPh_4 (342 mg, 1.00 mmol) to a solution of **2-ClO₄** (104 mg, 0.100 mmol) in methanol (40 mL). The resulting green solid was recrystallized from a mixed ethanol/acetonitrile solution. Yield: 101 mg (80%). M.p. 298–300 °C (decomp.). UV/Vis (CH_3CN): λ_{max} (ϵ) = 385 (2500), 649 (34), 1115 nm ($68 \text{ M}^{-1}\text{cm}^{-1}$). IR (KBr): $\tilde{\nu}$ = 1601 cm^{-1} , 1580 w, 1564 s [$\nu_{\text{as}}(\text{RCO}_2^-)$], 1423 [$\nu_{\text{s}}(\text{RCO}_2^-)$], 732, 703 (BPh_4^-). $\text{C}_{69}\text{H}_{88}\text{BClN}_6\text{Ni}_2\text{O}_2\text{S}_2$ (1261.3): calcd. C 65.71, H 7.03, N 6.66, S 5.08; found C 65.26, H 7.23, N 6.55, S 5.04. The tetraphenylborate salt **2-BPh₄** was additionally characterized by X-ray crystallography.

$[(\text{L}^2)\text{Ni}_2(m\text{-Cl-OBz})]\text{ClO}_4$ (3-ClO₄**). Method A (Oxidation with *meta*-Chloroperoxybenzoic acid, MCPBA):** A solution of *meta*-chloroperoxybenzoic acid (121 mg, 0.700 mmol) in acetonitrile (2 mL) was added dropwise to a solution of the perchlorate salt **2-ClO₄** (104 mg, 0.100 mmol) in acetonitrile (30 mL). During the addition the temperature was kept at 0 °C. After stirring for 2 h, a solution of $\text{LiClO}_4 \cdot 3\text{H}_2\text{O}$ (500 mg, 3.12 mmol) in ethanol (40 mL) was added. The product precipitated during evaporation of the solvent (the final amount of solvent was 3–4 mL). The pale-green microcrystalline material was isolated by filtration and dried in air. Yield: 95 mg (84%). M.p. 348–350 °C (decomp.). UV/Vis (CH_3CN): λ_{max} (ϵ) = 400 (47), 674 (16), 1126 nm ($15 \text{ M}^{-1}\text{cm}^{-1}$). IR (KBr): $\tilde{\nu}$ = 1606 cm^{-1} , 1563 s [$\nu_{\text{as}}(\text{RCO}_2^-)$], 1410 s [$\nu_{\text{s}}(\text{RCO}_2^-)$], 1220 vs [$\nu(\text{RSO}_3^-)$], 1091 vs [$\nu(\text{ClO}_4^-)$]. $\text{C}_{45}\text{H}_{68}\text{Cl}_2\text{N}_6\text{Ni}_2\text{O}_{12}\text{S}_2 \cdot 2\text{H}_2\text{O} \cdot \text{EtOH}$ (1137.5 + 82.1): calcd. C 45.61, H 6.52, N 6.79, S 5.18; found C 46.00, H 6.82, N 6.89, S 4.77. The tetraphenylborate salt $[(\text{L}^2)\text{Ni}_2(m\text{-Cl-OBz})]\text{BPh}_4$ (**3-BPh₄**) was prepared by adding NaBPh_4 (342 mg, 1.00 mmol) to a solution of **3-ClO₄** (114 mg, 0.100 mmol) in methanol (40 mL). The resulting pale-green solid was recrystallized from a mixed ethanol/acetonitrile solution. Yield: 128 mg (94%). M.p. 340–344 °C (decomp.). IR (KBr): $\tilde{\nu}$ = 1608 cm^{-1} , 1565 s [$\nu_{\text{as}}(\text{RCO}_2^-)$], 1410 w [$\nu_{\text{s}}(\text{RCO}_2^-)$], 1218 vs [$\nu(\text{RSO}_3^-)$], 732, 705 s [$\nu(\text{BPh}_4^-)$]. $\text{C}_{69}\text{H}_{88}\text{BClN}_6\text{Ni}_2\text{O}_8\text{S}_2 \cdot 2\text{H}_2\text{O}$ (1357.3 + 36.0): calcd. C 59.48, H 6.66, N 6.03, S 4.60; found C 59.47, H 6.92, N 5.82, S 3.97.

Method B (Oxidation with Hydrogen Peroxide): Hydrogen peroxide (1.00 mL, 35 wt.-% solution in water, 11.7 mmol) was added to a solution of **2-ClO₄** (104 mg, 0.10 mmol) in methanol (30 mL). The reaction mixture was refluxed for 5 h to give a pale-green solution. After cooling to room temperature, a solution of $\text{LiClO}_4 \cdot 3\text{H}_2\text{O}$ (0.500 g, 3.12 mmol) in ethanol (40 mL) was added. The product precipitated during evaporation of the solvent (the final amount of solvent was 3–4 mL). The pale-green microcrystalline material was isolated by filtration and dried in air. Yield: 70 mg (60%). The analytical data of this material are identical to those of compound **3-ClO₄** prepared by method A. The tetraphenylborate salt was additionally characterized by X-ray crystallography.

$[(\text{L}^2)\text{Ni}_2(\text{Cl})]\text{ClO}_4$ (4-ClO₄**):** H_2O_2 (1.00 mL, 35 wt.-% solution in water, 11.7 mmol) was added to a solution of **1-ClO₄** (92 mg, 0.10 mmol) in methanol (30 mL). The reaction mixture was refluxed for 4 h to give a pale-green solution. After cooling to room temperature, a solution of $\text{LiClO}_4 \cdot 3\text{H}_2\text{O}$ (0.250 g, 1.56 mmol) in ethanol (40 mL) was added. The product precipitated during evaporation of the solvent (the final amount of solvent was 3–4 mL). The pale-green microcrystalline material was isolated by filtration and dried in air. Yield: 63 mg (62%). An analytical sample was obtained by recrystallization from acetonitrile/ethanol. M.p. 318–320 °C (decomp.). UV/Vis (CH_3CN): λ_{max} (ϵ) = 396 (33), 686

(15), 1124 nm ($17 \text{ M}^{-1}\text{cm}^{-1}$). IR (KBr): $\tilde{\nu}$ = 1202 vs cm^{-1} [$\nu(\text{RSO}_3^-)$], 1092s [$\nu(\text{ClO}_4^-)$]. $\text{C}_{38}\text{H}_{64}\text{Cl}_2\text{N}_6\text{Ni}_2\text{O}_{10}\text{S}_2 \cdot 2\text{H}_2\text{O} \cdot \text{EtOH}$ (1017.4 + 82.1): calcd. C 43.70, H 6.78, N 7.64, S 5.83; found C 43.35, H 6.98, N 7.88, S 5.47. The tetraphenylborate salt $[(\text{L}^2)\text{Ni}_2(\text{Cl})]\text{BPh}_4$ (**4-BPh₄**) was prepared by adding NaBPh_4 (342 mg, 1.00 mmol) to a solution of **4-ClO₄** (105 mg, 0.100 mmol) in methanol (40 mL). The resulting green solid was recrystallized from a mixed ethanol/acetonitrile solution. Yield: 111 mg (90%). M.p. 330–334 °C (decomp.). IR (KBr): $\tilde{\nu}$ = 1203 vs cm^{-1} [$\nu(\text{RSO}_3^-)$]. $\text{C}_{62}\text{H}_{84}\text{BClN}_6\text{Ni}_2\text{O}_6\text{S}_2 \cdot \text{EtOH}$ (1237.2 + 46.1): calcd. C 59.90, H 7.07, N 6.55, S 5.00; found C 60.27, H 6.86, N 6.61, S 4.96. The tetraphenylborate salt was additionally characterized by X-ray crystallography. The oxidation of **1-ClO₄** by *meta*-chloroperoxybenzoic acid yields **3-ClO₄** (vide supra).

$[(\text{L}^2)\text{Ni}_2(\text{OAc})]\text{ClO}_4$ (6-ClO₄**). Method A (Oxidation with *meta*-Chloroperoxybenzoic Acid):** A solution of the acetato-bridged complex **5-ClO₄** (94 mg, 0.10 mmol) in acetonitrile (30 mL) was added slowly to a solution of *meta*-chloroperoxybenzoic acid (0.12 g, 0.70 mmol) in acetonitrile (2 mL). During the addition the temperature was kept at 0 °C. After stirring for 30 min, a solution of $\text{LiClO}_4 \cdot 3\text{H}_2\text{O}$ (0.500 g, 3.12 mmol) in ethanol (40 mL) was added. The product precipitated during evaporation of the solvent (the final amount of solvent was 3–4 mL). The pale-green microcrystalline material was isolated by filtration and dried in air. Yield: 87 mg (84%). M.p. 344–348 °C (decomp.). UV/Vis (CH_3CN): λ_{max} (ϵ) = 398 (55), 670 (25), 1122 nm ($47 \text{ M}^{-1}\text{cm}^{-1}$). IR (KBr): $\tilde{\nu}$ = 1611 sh cm^{-1} , 1597 s [$\nu_{\text{as}}(\text{RCO}_2^-)$], 1411 w [$\nu_{\text{s}}(\text{RCO}_2^-)$], 1202 vs [$\nu(\text{RSO}_3^-)$], 1092 s [$\nu(\text{ClO}_4^-)$]. $\text{C}_{40}\text{H}_{67}\text{ClN}_6\text{Ni}_2\text{O}_{12}\text{S}_2 \cdot 4\text{H}_2\text{O}$ (1041.0 + 72.1): calcd. C 43.16, H 6.79, N 7.55, S 5.76; found C 43.73, H 6.94, N 7.43, S 5.34.

Method B (Oxidation by Hydrogen Peroxide): Hydrogen peroxide (1.00 mL, 35 wt.-% solution in water, 11.7 mmol) was added to a solution of **5-ClO₄** (94 mg, 0.10 mmol) in methanol (30 mL). The reaction mixture was refluxed for 5 h to give a pale-green solution. After cooling to room temperature, a solution of $\text{LiClO}_4 \cdot 3\text{H}_2\text{O}$ (0.500 g, 3.12 mmol) in ethanol (40 mL) was added. The product precipitated during evaporation of the solvent (the final amount of solvent was 3–4 mL). The pale-green microcrystalline material was isolated by filtration and dried in air. Yield: 56 mg (50%). The analytical data of this material are identical to those of compound **6-ClO₄** prepared by method A.

Method C (from the Free Ligand $\text{H}_2\text{L}^2 \cdot 6\text{HCl}$): The reaction of $\text{Ni}(\text{OAc})_2 \cdot 4\text{H}_2\text{O}$ with $\text{H}_2\text{L}^2 \cdot 6\text{HCl}$ in the presence of a base also gives **6-ClO₄**. The procedure is detailed below for the corresponding zinc complex **8**.

$\text{H}_2\text{L}^2 \cdot 6\text{HCl}$: Hydrochloric acid (12 M, 100 mL) was added to a suspension of complex **3-ClO₄** (3.50 g, 3.08 mmol) in methanol (300 mL) and the reaction mixture was stirred vigorously at 50 °C for 24 h. The resulting solution was then concentrated at reduced pressure (final volume ca 40 mL) and the pH adjusted to 13 with 5 M aqueous potassium hydroxide solution. The resulting green suspension was allowed to cool to room temperature, and the aqueous phase was extracted with dichloromethane ($5 \times 100 \text{ mL}$). The organic fractions were combined and the dichloromethane was distilled off at reduced pressure to give a colorless solid. The residue was redissolved in ethanol (100 mL), acidified to pH 1 with conc. hydrochloric acid (ca. 3–4 mL), and the resulting solution quickly filtered off from an insoluble white solid (KCl). Evaporation of the solvent gave $\text{H}_2\text{L}^2 \cdot 6\text{HCl}$ as a colorless voluminous solid. M.p. 240–242 °C (dec.). Yield: 2.63 g (85%). This material was pure enough for metal-complex synthesis. IR (KBr): $\tilde{\nu}$ = 3023 w cm^{-1} , 2962 m, 2591 br. s, 1634, 1602, 1464 s, 1228 vs [$\nu(\text{RSO}_3 \text{ H})$], 1074

s, 1019 s, 688 s, 662 s. $C_{38}H_{72}Cl_6N_6O_6S_2$ (H_2O)₃ (985.86 + 54.05): calcd. C 43.89, H 7.65, N 8.08, S 6.17; found C 44.02, H 7.37, N 7.75, S 5.91. 1H NMR (200 MHz, D_2O , 330 K): δ = 7.87 (s, 4 H, ArH), 4.86 (s, 8 H, ArCH₂), 3.72 (t, 3J , 5.6 Hz, 8 H, CH₂), 3.33 (t, 3J , 5.6 Hz, 8 H, CH₂), 3.02 (s, 12 H, BzNCH₃), 2.45 (s, 6 H, NCH₃), 1.47 [s, 18 H, C(CH₃)₃] ppm. $^{13}C\{^1H\}$ NMR (50 MHz, D_2O): δ = 30.9 [C(CH₃)₃], 35.4 [C(CH₃)₃], 41.5 (CH₃), 52.5 (CH₂), 52.9 (CH₂), 60.9 (CH₂), 128.6, 136.0 (CH), 142.2, 157.4 ppm; one aliphatic carbon signal was not observed.

[(L³)Zn₂(OAc)(ClO₄)(8-ClO₄): Zn(O₂CCH₃)₂·2H₂O (44 mg, 0.20 mmol) and triethylamine (61 mg, 0.60 mmol) were added to a solution of H₂L²·6HCl (99 mg, 0.10 mmol) in methanol (25 mL). After stirring the reaction mixture for 2 d at room temperature, solid LiClO₄·3H₂O (321 mg, 2.00 mmol) was added. The mixture was then stirred for a further 12 h. The resulting white precipitate was collected by filtration and recrystallized from an acetonitrile/ethanol mixed-solvent system. Yield: 96 mg (91%). M.p. 360–364°C (decomp.). IR (KBr): $\tilde{\nu}$ = 1595 s cm⁻¹ [$\nu_{as}(\text{RCO}_2^-)$], 1411 w [$\nu_s(\text{RCO}_2^-)$], 1202 vs [$\nu(\text{RSO}_3^-)$], 1090 s [$\nu(\text{ClO}_4^-)$]. 1H NMR (200 MHz, CD₃OD): δ = 7.26 (s, 4 H, ArH), 4.58 (d, 2J = 12.4 Hz, 4 H, ArCH₂), 3.00 (d, 2J = 12.4 Hz, 4 H, ArCH₂), 2.95–2.75 (m, 16 H, CH₂), 2.68 (s, 6 H, NCH₃), 2.47 (s, 12 H, NCH₃), 1.26 [s, 18 H, C(CH₃)₃], 0.59 (s, 3 H, CH₃) ppm. $^{13}C\{^1H\}$ NMR (50 MHz, CDCl₃): δ = 173.1, 153.2, 143.5, 133.3, 132.5, 64.4, 57.1, 52.8, 45.3, 44.7, 35.08, 30.9, 23.3 ppm. C₄₀H₆₇ClN₆O₁₂S₂Zn₂·4H₂O (1054.4 + 72.1): calcd. C 42.65, H 6.71, N 7.46, S 5.69; found C 42.58, H 6.74, N 7.36, S 5.20.

[(L³)Cu₂(ClO₄)₂ (9·2ClO₄): [Cu(CH₃CN)₄]ClO₄ (65 mg, 0.20 mmol) and triethylamine (81 mg, 0.80 mmol) were added successively to a suspension of H₂L¹·6HCl (89 mg, 0.10 mmol) in methanol (40 mL). The colorless reaction mixture was stirred for 24 h and was then exposed to air to give a dark-green solution. A solution of LiClO₄·3H₂O (160 mg, 1.00 mmol) in methanol was added. The mixture was then filtered and stored in an open vessel for five days. The resulting green crystals were isolated by filtration and

dried in air. Yield: 45 mg (45%). M.p. 350–352°C (decomp.). IR (KBr): $\tilde{\nu}$ = 1058 cm⁻¹, 970 [$\nu(\text{RSO}_2^-)$], 1090 s [$\nu(\text{ClO}_4^-)$]. UV/Vis (CH₃CN): λ_{max} (ϵ) = 668 (430), 947 sh nm (153 M⁻¹cm⁻¹). C₃₈H₆₄Cl₂Cu₂N₆O₈S₂ (995.08): calcd. C 45.87, H 6.48, N 8.45, S 6.44; found C 45.66, H 6.53, N 8.33, S 6.22. This compound was additionally characterized by X-ray crystallography.

Crystal Structure Determinations: Single crystals of 2·BPh₄·1.25CH₃CN, 3·BPh₄·4EtOH·2H₂O, and 4·BPh₄·EtOH·0.5CH₃CN suitable for X-ray structure analysis were grown from an acetonitrile/ethanol (1:1) mixed-solvent system. Crystals of 9·(ClO₄)₂·H₂O were grown from methanolic solution. The crystals were mounted on glass fibers in perfluoropolyether oil. Intensity data were collected at 210(2) K, using a Bruker SMART CCD diffractometer. Graphite-monochromated Mo- K_α radiation (λ = 0.71073 Å) was used throughout. The data were processed with SAINT and corrected for absorption using SADABS^[47] (transmission factors: 1.00–0.89 for 2, 1.00–0.58 for 3, 1.00–0.85 for 4, and 1.00–0.91 for 9). The structures were solved by direct methods using the program SHELXS-86^[48] and refined by full-matrix least-squares techniques against F^2 using SHELXL-97.^[49] The ShelXTL version 5.10 program package was used for the structure solutions and refinements.^[50] PLATON was used to search for higher symmetry.^[51] Ortep3 was used for the artwork of the structures.^[52] Unless otherwise noted all non-hydrogen atoms were refined anisotropically. Hydrogen atoms were assigned to idealized positions and given isotropic thermal parameters 1.2-times (1.5-times for CH₃ groups) the thermal parameter of the atoms to which they are attached. Selected details of the data collection and refinement are given in Table 4.

In the crystal structure of 2 two *tert*-butyl groups were found to be disordered over two positions. A split-atom model was applied for the disordered *t*Bu groups. The site occupancies of the two orientations were refined as 0.70(1)/0.30(1) [for C(32a/c), C(33a/c), C(34a/c)] and 0.62(1)/0.38(1) [for C(36a/c), C(37a/c), C(38a/c)]. All non-hydrogen atoms were refined anisotropically, except the nitro-

Table 4. Crystallographic data for 2·BPh₄·1.25MeCN, 3·BPh₄·4EtOH·2H₂O, 4·BPh₄·EtOH·0.5CH₃CN, and 9·(ClO₄)₂·H₂O

Compound	2·BPh ₄ ·1.25MeCN	3·BPh ₄ ·4EtOH·2H ₂ O	4·BPh ₄ ·EtOH·0.5CH ₃ CN	9·(ClO ₄) ₂ ·H ₂ O
Formula	C _{71.5} H _{91.75} BClN _{7.25} Ni ₂ O ₈ S ₂	C ₇₇ H ₁₁₆ BClN ₆ Ni ₂ O ₁₄ S ₂	C ₆₅ H _{91.5} BClN _{6.5} Ni ₂ O ₇ S ₂	C ₃₈ H ₆₈ Cl ₂ Cu ₂ N ₆ O ₁₄ S ₂
M_r (g/mol)	1312.57	1577.56	1303.75	1095.08
Space group	$P\bar{1}$	$C2/c$	$P2_1/c$	$P2_1/c$
a (Å)	13.003(3)	31.604(6)	19.960(4)	12.688(3)
b (Å)	15.939(3)	16.444(4)	19.772(4)	9.131(2)
c (Å)	33.871(7)	34.628(6)	33.322(7)	20.780(4)
α (°)	77.22(3)	90.00	90.00	90.00
β (°)	82.06(3)	111.02(2)	93.514(5)	106.25(3)
γ (°)	82.75(3)	90.00	90.00	90.00
V (Å ³)	6747(2)	16798(6)	13126(5)	2311.3(9)
Z	4	8	8	2
$d_{\text{calcd.}}$ (g/cm ³)	1.292	1.248	1.319	1.574
Cryst. size (mm ³)	0.30 × 0.30 × 0.30	0.20 × 0.26 × 0.31	0.30 × 0.30 × 0.20	0.20 × 0.20 × 0.20
$\mu(\text{Mo-}K_\alpha)$ (mm ⁻¹)	0.710	0.591	0.734	1.197
2 θ limits (deg)	2.64–58.14	1.52–57.66	3.10–57.76	3.34–56.60
Measured refl.	61676	42079	81701	14432
Independent refl.	31611	18414	31159	5571
Observed refl. ^[a]	12737	5500	12272	3025
No. parameters	1608	802	1519	289
$R1^{[b]}$ ($R1$ all data)	0.0533 (0.1054)	0.0783 (0.1996)	0.0554 (0.1378)	0.0446 (0.0969)
$wR2^{[c]}$ ($wR2$ all data)	0.1639 (0.1410)	0.2458 (0.2737)	0.1696 (0.1784)	0.1032 (0.1153)
Max., min. peaks (e/Å ³)	0.724, -0.831	1.309, -1.219	1.237, -1.160	0.591, -0.565

[a] Observation criterion: $I > 2\sigma(I)$. [b] $R1 = \sum ||F_o| - |F_c|| / \sum |F_o|$. [c] $wR2 = \{\sum [w(F_o^2 - F_c^2)^2] / \sum [w(F_o^2)^2]\}^{1/2}$.

gen and carbon atoms [N(9), C(51), C(52)] of one half-occupied acetonitrile solvent molecule. No hydrogen atoms were calculated for the methyl carbon atom C(52). In the crystal structure of **3**, the C and O atoms of the ethanol and water molecules of solvent of crystallization were found to exhibit very large thermal parameters indicative of severe disorder. This disorder could not be modeled by using split-atom models, therefore the coordinates of the respective atoms were fixed at their initial positions and given a common isotropic thermal parameter of 0.20. No problems were encountered with the refinement of the $[(L^2)Ni_2(m-Cl-OBz)]^+$ cation. The relatively large *R* value is due to the disorder of the solvent molecules. In the crystal structure of **4**, one *tert*-butyl group and the two ethanol molecules of crystallization were found to be disordered over two positions. A split atom model was applied to account for this disorder. The site occupancies of the two orientations were refined as 0.53(1)/0.47(1) [for C(32a/b), C(33a/b), C(34a/b)], 0.71(1)/0.29(1) [for O(5a/b), C(39a/b), C(40a/b)], and 0.78(1)/0.22(1) [for O(7a/b), C(41a/b), C(42a/b)]. The disorder of the acetonitrile molecule of solvent of crystallization could not be modeled by using a split-atom model, therefore the coordinates of the C and N atoms were fixed at their initial positions and given a common isotropic thermal parameter of 0.20. No hydrogen atoms were calculated for the solvate molecules. In the crystal structure of **9**·(ClO₄)₂(H₂O) no hydrogen atoms were calculated for the H₂O molecule.

CCDC-239553 (for **2**), -239554 (for **3**), -239555 (for **4**) and -239556 (for **9**) contain the supplementary crystallographic data for this paper. These data can be obtained free of charge via www.ccdc.cam.ac.uk/conts/retrieving.html (or from the Cambridge Crystallographic Data Centre, 12 Union Road, Cambridge CB2 1EZ, UK (fax: +44-1223-336-033; or deposit@ccdc.cam.ac.uk)).

Calculation of Ring-Current Effects: All ab initio calculations were performed on an SGI Octane and an SGI Origin 2000 using the program Gaussian 98.^[53] Geometry optimization was carried out using HF/6-31G* without restrictions.^[54] The chemical shieldings in the surrounding of the molecules were calculated based on the idea of NICS (nucleus-independent chemical shift) by Schleyer.^[55] The molecule was placed in the center of a grid of “ghost atoms” ranging from −10.0 to +10.0 Å in all three dimensions with a step width of 0.5 Å. This resulted in a cube of 68921 ghost atoms. The chemical-shielding calculations were done with the GIAO (gauge-independent atomic orbital) method using HF/6-31G*.^[56] Since GIAO is a coupled HF method that uses gauge-independent atom orbitals for the calculation of shielding values it can be applied in the calculation of NICS. From the GIAO calculations the coordinates and isotropic shielding values of the ghost atoms were extracted. After the transformation of the tabulated chemical shieldings into a SYBYL contour file, the ring-current effects of the two isolated phenyl rings in the complexes can be visualized as iso chemical-shielding surfaces (ICSS).^[57] Thus, it is possible to map both spatial extension and sign of the ring current effects of the two phenyls on the methyl protons at each position.^[58]

The chemical shielding values at the positions of the three methyl protons of the bridging acetate ions in **7** and **8** (atomic coordinates were taken from the crystal structures) were calculated as follows: **7**: $\Delta\delta = -1.56, -1.08, -1.12$ ppm (mean value = −1.25 ppm, in the gas phase); **8**: $\Delta\delta = -2.32, -1.59, -1.85$ ppm (mean value = −1.92 ppm). The observed chemical shielding values (relative to NaOAc at $\delta = 1.83$ ppm in CD₃OD) are as follows: **7** $\delta(\mu\text{-OAc}) = 0.86$ ppm ($\Delta\delta = -0.97$ ppm); **8**: $\delta(\mu\text{-OAc}) = 0.59$ ppm ($\Delta\delta = -1.24$ ppm). The differences between the calculated and the experimental values are most likely due to solvation effects.

Supporting Information Available: Figures S1 and S2 (see also the footnote on the first page of this article). The calculated chemical shielding values at the positions of the three methyl protons of the bridging acetate ions in **7** and **8**.

Acknowledgments

We are particularly grateful to Prof. Dr. H. Vahrenkamp for providing facilities for NMR and X-ray crystallographic measurements. Financial support of this work from the Deutsche Forschungsgemeinschaft (Priority programme “Sekundäre Wechselwirkungen”, KE 585/3-1,2) and by the Wissenschaftliche Gesellschaft in Freiburg is gratefully acknowledged.

- [1] J. W. Canary, B. C. Gibb, *Prog. Inorg. Chem.* **1997**, *45*, 1–83.
- [2] C. Wieser, C. B. Dieleman, D. Matt, *Coord. Chem. Rev.* **1997**, *165*, 93–161.
- [3] S. Hecht, J. M. J. Fréchet, *Angew. Chem.* **2001**, *113*, 76–94; *Angew. Chem. Int. Ed.* **2001**, *40*, 74–91.
- [4] [4a] M. T. Reetz, S. R. Waldvogel, *Angew. Chem.* **1997**, *109*, 870–873; *Angew. Chem. Int. Ed. Engl.* **1997**, *36*, 865–867. [4b] M. T. Reetz, *Catal. Today* **1998**, *42*, 399.
- [5] E. Engeldinger, D. Armspach, D. Matt, *Angew. Chem.* **2001**, *113*, 2594–2597; *Angew. Chem. Int. Ed.* **2001**, *40*, 2526–2529.
- [6] V. F. Slagt, J. N. H. Reek, P. C. J. Kramer, P. W. N. M. van Leeuwen, *Angew. Chem.* **2001**, *113*, 4401–4404; *Angew. Chem. Int. Ed.* **2001**, *40*, 4271–4274.
- [7] M. Yoshizawa, Y. Takeyama, T. Kusukawa, M. Fujita, *Angew. Chem.* **2002**, *114*, 1403–1405; *Angew. Chem. Int. Ed.* **2002**, *41*, 1347–1349.
- [8] T. Ooi, Y. Kondo, K. Maruoka, *Angew. Chem.* **1998**, *110*, 3213–3215; *Angew. Chem. Int. Ed.* **1998**, *37*, 3039–3041.
- [9] [9a] S. Blanchard, L. Le Clainche, M.-N. Rager, B. Chansou, J.-P. Tuchagues, A. F. Duprat, Y. Le Mest, O. Reinaud, *Angew. Chem.* **1998**, *110*, 2861–2864; *Angew. Chem. Int. Ed.* **1998**, *37*, 2732–2735. [9b] Y. Rondelez, G. Bertho, O. Reinaud, *Angew. Chem.* **2002**, *114*, 1086–1088; *Angew. Chem. Int. Ed.* **2002**, *41*, 1044–1046. [9c] Y. Rondelez, M.-N. Rager, A. Duprat, O. Reinaud, *J. Am. Chem. Soc.* **2002**, *124*, 1334–1340. [9d] O. Seneque, M.-N. Rager, M. Giorgi, O. Reinaud, *J. Am. Chem. Soc.* **2001**, *123*, 8442–8443. [9e] O. Seneque, M.-N. Rager, M. Giorgi, O. Reinaud, *J. Am. Chem. Soc.* **2000**, *122*, 6183–6189.
- [10] B. R. Cameron, S. J. Loeb, G. P. A. Yap, *Inorg. Chem.* **1997**, *36*, 5498–5504.
- [11] For reviews of cyclodextrins, see *Chem. Rev.* **1998**, *98*, 1741–2076 (special issue).
- [12] [12a] N. Kitajima, W. B. Tolman, *Prog. Inorg. Chem.* **1995**, *43*, 419–531. [12b] S. Trofimenko, *Scorpionates: The Coordination Chemistry of Polypyrazolylborate Ligands*, Imperial College Press, London, U.K., **1999**. [12c] H. Vahrenkamp, *Acc. Chem. Res.* **1999**, *32*, 589–596.
- [13] P. Chaudhuri, K. Wieghardt, *Prog. Inorg. Chem.* **1988**, *35*, 329–436.
- [14] B. S. Hammes, D. Ramos-Maldonado, G. P. A. Yap, L. Liable-Sands, A. L. Rheingold, V. G. Young Jr., A. S. Borovik, *Inorg. Chem.* **1997**, *36*, 3210–3211.
- [15] A. J. Atkins, D. Black, A. J. Blake, A. Marin-Becerra, S. Parsons, L. Ruiz-Ramirez, M. Schröder, *Chem. Commun.* **1996**, 457–464.
- [16] J. B. Fontecha, S. Goetz, V. McKee, *Angew. Chem.* **2002**, *114*, 4735–4738; *Angew. Chem. Int. Ed.* **2002**, *41*, 4553–4556.
- [17] T. Kajiwara, H. Wu, T. Ito, N. Iki, S. Miyano, *Angew. Chem.* **2004**, *116*, 1868–1871; *Angew. Chem. Int. Ed.* **2004**, *43*, 1832–1835.
- [18] [18a] A. J. Atkins, A. J. Blake, M. Schröder, *J. Chem. Soc., Chem. Commun.* **1993**, 1662–1665. [18b] N. D. J. Branscombe, A. J. Blake, A. Marin-Becerra, W.-S. Li, S. Parsons, L. Ruiz-Ramirez, M. Schröder, *Chem. Commun.* **1996**, 2573–2574.

- [19] [19a] S. Brooker, P. D. Croucher, *J. Chem. Soc., Chem. Commun.* **1995**, 1493–1494. [19b] S. Brooker, P. D. Croucher, *J. Chem. Soc., Chem. Commun.* **1995**, 2075–2076. [19c] S. Brooker, P. D. Croucher, F. M. Roxburgh, *J. Chem. Soc., Dalton Trans.* **1996**, 3031–3037. [19d] S. Brooker, P. D. Croucher, *Chem. Commun.* **1997**, 459–460. [19e] S. Brooker, P. D. Croucher, T. C. Davidson, G. S. Dunbar, A. J. McQuillan, G. B. Jameson, *Chem. Commun.* **1998**, 2131–2132.
- [20] N. H. Pilkington, R. Robson, *Aust. J. Chem.* **1970**, *23*, 2225–2236.
- [21] [21a] P. A. Vigato, S. Tamburini, D. Fenton, *Coord. Chem. Rev.* **1990**, *106*, 25–170. [21b] D. Fenton, *Chem. Soc., Rev.* **1999**, *28*, 159–168.
- [22] [22a] H. Okawa, H. Furutachi, D. E. Fenton, *Coord. Chem. Rev.* **1998**, *174*, 51–75. [22b] M. Shinoura, S. Kita, M. Ohba, H. Okawa, H. Furutachi, M. Suzuki, *Inorg. Chem.* **2000**, *39*, 4520–4526.
- [23] [23a] C. Fraser, L. Johnston, A. L. Rheingold, B. S. Haggerty, G. K. Williams, J. Whelan, B. Bosnich, *Inorg. Chem.* **1992**, *31*, 1835–1844. [23b] B. Bosnich, *Inorg. Chem.* **1999**, *38*, 2554–2562. [23c] A. L. Gavrilova, C. J. Qin, R. D. Sommer, A. L. Rheingold, B. Bosnich, *J. Am. Chem. Soc.* **2002**, *124*, 1714–1722.
- [24] [24a] B. Kersting, G. Steinfeld, *Chem. Commun.* **2001**, 1376–1377. [24b] M. H. Klingele, G. Steinfeld, B. Kersting, *Z. Naturforsch., Teil B* **2001**, *56*, 901–907. [24c] B. Kersting, G. Steinfeld, *Inorg. Chem.* **2002**, *41*, 1140–1150.
- [25] B. Kersting, *Angew. Chem.* **2001**, *113*, 4109–4112; *Angew. Chem. Int. Ed.* **2001**, *40*, 3987–3990.
- [26] I. K. Adzhamli, K. Libson, J. D. Lydon, R. C. Elder, E. Deutsch, *Inorg. Chem.* **1979**, *18*, 303–311.
- [27] [27a] C. A. Grapperhaus, M. Y. Darensbourg, *Acc. Chem. Res.* **1998**, *31*, 451–459. [27b] R. M. Buonomo, I. Font, M. J. Maguire, J. H. Reibenspies, T. Tuntulani, M. Y. Darensbourg, *J. Am. Chem. Soc.* **1995**, *117*, 963–973.
- [28] S. A. Mirza, M. A. Pressler, M. Kumar, R. O. Day, M. J. Maroney, *Inorg. Chem.* **1993**, *32*, 977–987.
- [29] [29a] V. E. Kaasjager, E. Bouwman, S. Gorter, J. Reedijk, C. A. Grapperhaus, J. H. Reibenspies, J. J. Smee, M. Y. Darensbourg, A. Dereskei-Kovacs, L. M. Thomson, *Inorg. Chem.* **2002**, *41*, 1837–1844. [29b] R. K. Henderson, E. Bouwman, A. L. Spek, J. Reedijk, *Inorg. Chem.* **1997**, *36*, 4616–4617.
- [30] The absence of sharp ^1H NMR resonances in the $\delta = 0$ –10 ppm region indicates that the nickel complexes **1**–**6** are paramagnetic in solution. For complexes **2** and **5** this is further supported by temperature-dependent magnetic susceptibility measurements.^[45] We anticipate performing a more detailed study of the electronic structures of the other compounds by temperature-dependent susceptibility measurements.
- [31] Abbreviations: MCPBA = *meta*-chloroperoxybenzoic acid ($m\text{-Cl-C}_6\text{H}_4\text{-CO}_3\text{H}$), $m\text{-Cl-OBz} = m\text{-Cl-C}_6\text{H}_4\text{-CO}_2^-$, $\text{OAc}^- = \text{CH}_3\text{CO}_2^-$.
- [32] N. D. J. Branscombe, A. J. Atkins, A. Marin-Becerra, E. J. L. McInnes, F. E. Mabbs, J. McMaster, M. Schröder, *Chem. Commun.* **2003**, 1098–1099.
- [33] S. A. Mirza, R. O. Day, M. J. Maroney, *Inorg. Chem.* **1996**, *35*, 1992–1995.
- [34] G. Steinfeld, V. Lozan, B. Kersting, *Angew. Chem.* **2003**, *115*, 2363–2365; *Angew. Chem. Int. Ed.* **2003**, *42*, 2261–2263.
- [35] M. Y. Darensbourg, T. Tuntulani, J. H. Reibenspies, *Inorg. Chem.* **1995**, *34*, 6287–6294.
- [36] K. Nakamoto, *Infrared and Raman Spectra of Inorganic and Coordination Compounds*, 5th ed., Wiley-VCH, New York, **1997**.
- [37] For a complete listing of these IR absorptions see: Exp. Sect., complex **2**.
- [38] P. J. Farmer, T. Solouki, D. K. Mills, T. Soma, D. H. Russell, J. H. Reibenspies, M. Y. Darensbourg, *J. Am. Chem. Soc.* **1992**, *114*, 4601–4605.
- [39] The nickel complex **5** and other carboxylato-bridged dinickel complexes of $(\text{L}^1)^{2-}$ all display an intense absorption in the 380 to 400 nm region ($\epsilon \approx 2500 \text{ M}^{-1}\text{cm}^{-1}$) in CH_3CN solution.
- [40] M. Duggan, N. Ray, B. Hathaway, G. Tomlinson, P. Brint, K. Pelin, *J. Chem. Soc., Dalton Trans.* **1980**, 1342–1348.
- [41] See Supporting Information.
- [42] A preliminary crystal structure determination of **8-BPh₄** revealed the structure of the complex cation **8** to be very similar to that of **3**, with a $\text{Zn}\cdots\text{Zn}$ distance of 4.542(2) Å and an acute angle (41.6°) between the phenyl rings. However, due to severe disorder of the solvent molecules, the *R* value is very low and the structure cannot be published yet.
- [43] B. Kersting, *Z. Anorg. Allg. Chem.* **2004**, *630*, 765–780.
- [44] F. A. Cotton, G. Wilkinson, C. A. Murillo, M. Bochmann, *Advanced Inorganic Chemistry*, 6th ed., John Wiley & Sons, New York, **1999**, p. 492.
- [45] J. Hausmann, M. H. Klingele, V. Lozan, G. Steinfeld, D. Siebert, Y. Journaux, J. J. Girerd, B. Kersting, *Chem. Eur. J.* **2004**, *10*, 1716–1728.
- [46] J. Ackermann, F. Meyer, E. Kaifer, H. Pritzkow, *Chem. Eur. J.* **2002**, *8*, 247–258.
- [47] SADABS, An empirical absorption correction program part of the SAINTplus NT version 5.10 package, BRUKER AXS, Madison, WI, **1998**.
- [48] G. M. Sheldrick, *Acta Crystallogr., Sect. A* **1990**, *46*, 467–473.
- [49] G. M. Sheldrick, *SHELXL-97*, Computer program for crystal structure refinement, University of Göttingen, Göttingen, Germany, **1997**.
- [50] ShelXTL version 5.10: Bruker AXS, Madison, WI, **1998**.
- [51] A. L. Spek, *PLATON – A Multipurpose Crystallographic Tool*; Utrecht University, Utrecht, The Netherlands, **2000**.
- [52] L. J. Farrugia, *J. Appl. Cryst.* **1997**, *30*, 565.
- [53] Gaussian 98, Revision A.11.3: M. J. Frisch, G. W. Trucks, H. B. Schlegel, G. E. Scuseria, M. A. Robb, J. R. Cheeseman, V. G. Zakrzewski, J. A. Montgomery, Jr., R. E. Stratmann, J. C. Burant, S. Dapprich, J. M. Millam, A. D. Daniels, K. N. Kudin, M. C. Strain, O. Farkas, J. Tomasi, V. Barone, M. Cossi, R. Cammi, B. Mennucci, C. Pomelli, C. Adamo, S. Clifford, J. Ochterski, G. A. Petersson, P. Y. Ayala, Q. Cui, K. Morokuma, N. Rega, P. Salvador, J. J. Dannenberg, D. K. Malick, A. D. Rabuck, K. Raghavachari, J. B. Foresman, J. Cioslowski, J. V. Ortiz, A. G. Baboul, B. B. Stefanov, G. Liu, A. Liashenko, P. Piskorz, I. Komaromi, R. Gomperts, R. L. Martin, D. J. Fox, T. Keith, M. A. Al-Laham, C. Y. Peng, A. Nanayakkara, M. Challacombe, P. M. W. Gill, B. Johnson, W. Chen, M. W. Wong, J. L. Andres, C. Gonzalez, M. Head-Gordon, E. S. Replogle, J. A. Pople, Gaussian, Inc., Pittsburgh PA, **2002**.
- [54] W. J. Hehre, L. Radom, P. v. R. Schleyer, J. A. Pople, *Ab initio Molecular Orbital Theory*, Wiley New York, **1986**.
- [55] P. v. R. Schleyer, C. Maerker, A. Dansfeld, H. Jiao, N. J. R. v. E. Hommes, *J. Am. Chem. Soc.* **1996**, *118*, 6317–6318.
- [56] [56a] J. R. Ditchfield, *Mol. Phys.* **1974**, *27*, 789–807. [56b] J. P. Cheeseman, G. W. Trucks, T. A. Keith, M. J. Frisch, *J. Chem. Phys.* **1996**, *104*, 5497–5509.
- [57] SYBYL 6.9: Tripos Inc., St. Louis MO 63144, S. Hanley Road 303, **2002**.
- [58] S. Klod, E. Kleinpeter, *J. Chem. Soc., Perkin Trans. 2* **2001**, 1893–1898.

Received June 2, 2004

Early View Article

Published Online October 7, 2004